

Rolipram, a phosphodiesterase 4 inhibitor, prevented cancellous and cortical bone loss by inhibiting endosteal bone resorption and maintaining the elevated periosteal bone formation in adult ovariectomized rats

W. Yao¹, X.Y. Tian¹, J. Chen¹, R.B. Setterberg¹, M.W. Lundy², P. Chmielzowski², C.A. Froman², W.S.S. Jee¹

¹Radiobiology Division, University of Utah School of Medicine, Salt Lake City, Utah, USA;

²Bone Biology, Health Care Research, Procter & Gamble Pharmaceuticals, Mason, Ohio, USA

Abstract

Cyclic AMP (cAMP) is a continually produced nucleotide inactivated by hydrolysis to 5'AMP via phosphodiesterase (PDE) enzymes. Rolipram is a selective PDE4 inhibitor reported to have anti-inflammatory effects and used in the treatment of asthma and chronic obstructive pulmonary disease (COPD). The current study was designed to determine whether Rolipram could prevent and restore bone loss in ovariectomized (OVX) rats. Six-month-old Sprague Dawley rats underwent either sham-operated or bilateral ovariectomy, and were left untreated for 60 days to develop osteopenia. Then they were treated with vehicle, 6 mg/kg PGE₂, 3 µg/kg Alendronate or 0.1-1.0 mg/kg Rolipram for 60 days. At sacrifice, the right tibiae were processed for quantitative bone histomorphometric measurements. The right femurs were measured by dual energy X-ray absorptiometry and the 5th lumbar vertebrae were subjected to micro-computed tomography to access bone mass and architecture changes. Our results indicated that OVX induced negative bone balance in all five bone sites we tested, with bone resorption exceeding bone formation. Rolipram at 0.1-0.6 mg/kg dose levels prevented while at 1 mg/kg restored ovariectomy-induced cancellous and cortical bone loss in the tibia, femur and lumbar vertebra. Dynamic bone histomorphometry suggested that these beneficial effects were achieved by partially maintaining the elevated bone formation at the trabecular bone surface and increasing bone formation at the periosteal bone surface of the cortex. Furthermore, it reduced bone turnover at the trabecular and the endocortical bone surfaces. The prevention of further bone loss effects were comparable to those of an anti-resorption agent (Alendronate) but were not as great as those of an anabolic agent (PGE₂). In addition, Rolipram treatment increased body and muscle weights compared to the vehicle-treated OVX rats. In conclusion, our study in an osteopenic rat model suggested that a selective PDE4 inhibitor may be used for the treatment of established osteoporosis.

Keywords: Rolipram, Rat, Ovariectomy, Bone Histomorphometry, DEXA, Micro-CT

Introduction

Osteoporosis, a disease of bone fragility, is defined as low bone mass leading to vertebral and hip fractures¹. Most cur-

rent therapies involve the uses of anti-resorptive agents that slow bone turnover rates and result in a reduced remodeling space²⁻⁴. This method of therapy maintains bone mass at the existing level or increases bone mass up to approximately 10 percent. Larger increases in bone mass can be attained by using anabolic agents such as parathyroid hormone (PTH), sodium fluoride and prostaglandin E₂ (PGE₂) and basic fibroblast growth factor (bFGF)⁵⁻⁷. However, the use of these agents is limited by their side effects and/or the cumbersome mode of administration. Thus there is a need to search for new bone anabolic agents in addition to PTH that are easy to administer, have a good safety profile and are able to reduce fracture incidence beyond the level seen with currently available anti-resorptive treatment.

Authors Yao, Tian, Chen, Setterberg and Jee have no conflict of interest. Authors Lundy, Chmielzowski, and Froman have corporate appointments with Procter & Gamble Pharmaceuticals.

Corresponding author: Dr. Webster S.S. Jee, Division of Radiobiology, University of Utah, 729 Arapahoe Dr, Suite 2338, Salt Lake City, Utah 84108, USA
E-mail: webster.jee@hsc.utah.edu

Accepted 1 June 2006

Groups	Animal #	Treatment	Dose
1	6	Baseline control (Basal)	N/A
2	6	Pre-treatment intact (60d-Sham)	N/A
3	6	Final intact (120d-Sham)	Vehicle
4	6	Pre-treatment OVX (60d-OVX)	N/A
5	6	Final OVX (120d-OVX)	Vehicle
6	6	OVX+PGE ₂	6.0 mg/kg/d
7	6	OVX+Alendronate (Ale)	3.0 µg/kg/d
8	6	OVX+Rolipram (Rol-0.1)	0.1 mg/kg/d
9	6	OVX+Rolipram (Rol-0.3)	0.3 mg/kg/d
10	6	OVX+Rolipram (Rol-0.6)	0.6 mg/kg/d
11	6	OVX+Rolipram (Rol-1.0)	1.0 mg/kg/d

Table 1. Experimental design.

Groups	Gastrocnemius Weight (g)
Basal	^a 1.75±0.10
60d-Sham	^a 1.75±0.09
120d-Sham	^a 1.78±0.10
60d-OVX	1.95±0.09
120d-OVX	1.96±0.07
OVX+PGE ₂	1.78±0.14
OVX+Ale	1.81±0.25
OVX+Rol-0.1	2.12±0.11
OVX+Rol-0.3	^{abc} 2.17±0.17
OVX+Rol-0.6	^{abc} 2.35±0.12
OVX+Rol-1.0	^{abc} 2.25±0.14

Ale, Alendronate; Rol, Rolipram 0.1-1.0 mg/kg; ^a=*p*<0.05 from 60d-OVX and 120d-OVX; ^b=*p*<0.05 from PGE₂; and ^c=*p*<0.05 from Ale group.

Table 2. Muscle weight.

Phosphodiesterase (PDE) catalyzes the hydrolysis of cAMP and cGMP in cells^{8,9}. Since prostaglandins and other anabolic agents such as PGE₂ and PTH stimulate an increase in intracellular cAMP synthesis, decreasing the hydrolysis rate of these intracellular mediators might then increase cAMP level and result in a net increase in bone volume¹⁰⁻¹⁴. There are 11 known isozymes of PDE¹⁵. Variants in the gene encoding PDE4 account for some of the genetic contributions to bone mineral density variation in humans¹⁶. Recent studies suggested that using inhibitors of PDE4 increased bone volume in young rats, prevented bone loss in rats bearing carcinosarcoma or induced by estrogen-deficiency and added bone to growing mice^{17-19,21}. *In vitro* studies have suggested that PDE4 inhibitors act by inhibiting osteoclast-like cell formation and increasing osteoblast expressing RANKL mRNA and osteoblastogenesis^{20,21}. However, these few studies were limited to intact young growing mice or 6-8 week old rats. Questions arise whether the PDE4 inhibitor has the

same beneficial effects on the older rat skeleton (8-month-old) with established osteopenia following estrogen depletion. To address this issue, the current study was designed to test one of the PDE4 inhibitors, Rolipram, in rats that were 8 months of age and 2 months post-ovariectomy at the beginning of the treatment. Multiple skeletal sites including metaphysis and diaphysis of long and axial bones were evaluated in order to study if Rolipram might serve as a potential candidate for treatment of OVX-induced bone loss. In addition, we also compared the effects of Rolipram to an anti-resorptive agent, Alendronate and an anabolic agent, PGE₂.

Materials and methods

Experimental protocol

Sixty-eight female 3-month-old Sprague Dawley rats (Simonsen Laboratories, Gilroy, GA) were acclimated to local vivarium conditions. They were pair-fed in cages with the room temperature maintained at 72°F and 12:12 light/dark cycles. The rats were allowed free access to water and pelleted commercial natural diet (Teklad Rodent Laboratory Chow #8604, Harlan Teklad, Madison, WI) that contains 1.46% calcium, 0.99% phosphorus and 4.96 IU/g of vitamin D₃. Sham or bilateral ovariectomy was performed at 6 months of age. The rats were divided into 11 body weight-matched groups with 6 rats in each group (Table 1). Beginning 60 days after OVX operation, the rats were treated daily for 60 days with subcutaneous (sc.) 6 mg/kg PGE₂ injection (Cayman Chemicals, Ann Arbor, Michigan) that served as a positive anabolic control, sc. 3 µg/kg of Alendronate (Starks Associate, Inc., Buffalo, NY), sc., that served as a positive anti-resorptive control, or sc. 0.1-1.0 mg/kg of Rolipram (Research Biochemical International, Cincinnati, OH). Rolipram dose ranges were based on the HARBS/PDE4 ratio of prototype compounds, with references to the published papers on Rolipram^{19,21}. We chose to use lower Rolipram doses for the study to evaluate if we could achieve similar effects in this established osteopenic rat model. Two percent methyl cellulose at pH 7.4 phosphate buffered saline with 2% TWEEN 80 was used as vehicle injection. All the rats received 90 mg/kg of Xylenol Orange and 10 mg/kg of Calcein (Sigma Chemical Co., St. Louis, MO) on 14 and 4 days before sacrifice. At necropsy, the rats were anesthetized by an intraperitoneal injection of Ketamine (50 mg/kg) and Xylazine (10 mg/kg) and sacrificed by cardiac puncture. The right tibiae, femurs and the 5th lumbar vertebrae were harvested and analyzed by bone histomorphometry, by dual energy X-ray absorptiometer and micro-computed tomography, respectively.

Bone histomorphometry

The right proximal tibiae and the middle-third of the right tibiae were stained with Villanueva bone stain, dehydrated in graded concentrations of ethanol, defatted in acetone, and embedded in methyl methacrylate (Fisher Scientific, Fairlawn,

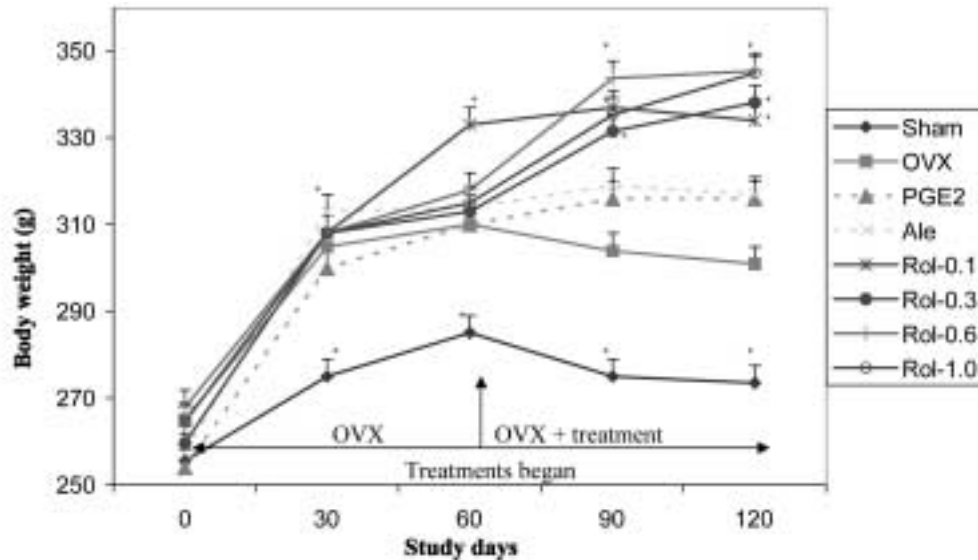


Figure 1. Body weight changes for the study. Body weights were higher in the ovariectomized (OVX) animals than in Sham-operated ones. PGE₂ and Alendronate (Ale) had similar body weights with the OVX animals. From 30 days after the treatment was initiated, Rolipram (Rol) at 0.6 mg and 1mg doses significantly increased body weights compared to OVX animals. *= $p < 0.05$ compared to the OVX group at the same timepoint.

NJ). Longitudinal sections of proximal tibiae (PT) and cross-sections at the tibiofibular junction of the tibial shafts (TX) were cut to 230 μm thickness using a low speed metallurgical saw and then ground to 20 μm (PT) and 30 μm (TX) for histomorphometric measurement. Histomorphometry was done with a semi-automatic image analysis system (OsteoMeasure, OsteoMetrics Inc., Decatur, GA) linked to a microscope equipped with transmission and fluorescence light.

The region of the proximal tibial metaphysis studied was from 1 mm to 4 mm distal to the growth plate-metaphyseal junction. Static measurements included total tissue area (T.Ar), bone area (B.Ar) and bone perimeter (B.Pm). Dynamic measurements included single- (sL.Pm) and double-labeled perimeter (dL.Pm), eroded perimeter (E.Pm), and interlabel width (Ir.L.Wi). These indices were used to calculate percentage trabecular bone area (B.Ar/T.Ar), trabecular number (Tb.N), trabecular width (Tb.Wi) and trabecular separation (Tb.Sp), percentage eroded perimeter (%E.Pm/B.Pm), mineral apposition rate (MAR), bone formation rate per unit of bone area (BFR/B.Ar), of total tissue area (BFR/T.Ar), of bone surface (BFR/B.Pm) and activation frequency (Ac.f) according to Parfitt et al.^{22,23}

Cortical bone measurements included total cross-sectional area (Tt.Ar), marrow area (Ma.Ar), eroded perimeter (E.Pm), single- and double-labeled perimeter (sL.Pm, dL.Pm), and interlabeled width (Ir.L.Wi). These parameters were used to calculate the cortical bone area (Ct.Ar), percentage cortical area (%Ct.Ar), percentage marrow area (%Ma.Ar), mineral apposition rate (MAR) and bone formation rate per bone surface (BFR/B.Pm) of the periosteal (Ps) and endocortical (Ec) bone surfaces according to Jee et al.²⁴.

Micro-computed tomography (μCT)

The 5th lumbar vertebral bodies were removed from all animals and were cleaned of soft tissue. The processes were removed and the vertebral bodies placed in 70% ethanol. Each lumbar vertebral body was imaged using a micro-computed tomography system (μCT 20, serial # 96-2004, Scanco Medical AG). The caudal end of the vertebra was placed on the left side of the holder alignment line to aid in consistent positioning of the bone. The samples were separated by a sponge material moistened with 70% ethanol, which acts to secure the vertebra in position and keeps the sample moist. Image acquisition parameters for the vertebra included standard resolution (300 projections), 26 μm slice increment, and 150 msec integration time. Approximately 186 slices were scanned per vertebra. Once acquisition was complete, the images were sent to a SGI Octane Workstation for all subsequent analyses. The image analysis involved: (a) setting the threshold of the images to bone and background; (b) determining of the volume of interest (VOI); (c) separating of the cortical from the trabecular bone; and (d) measuring of structural parameters, as described previously²⁵. Measurements made on the 3-D datasets included trabecular bone volume, trabecular thickness, trabecular number, trabecular separation, connectivity density, cortical thickness, star volume and percentage of plate-like trabeculae (% plate derived).

Dual energy X-ray absorptiometry (DEXA)

Bone mineral density (BMD) and bone mineral content (BMC) of the right femurs were determined *ex vivo* utilizing a dual-energy X-ray absorptiometer (DEXA), Hologic® QDR-

2000 plus bone densitometer (Hologic®, Inc., Waltham, MA). The scanning of small animal bones requires the use of the regional high-resolution software (with 0.0100 inch line spacing and 0.00499 inch point resolution). This software automatically selects a small X-ray source collimator (0.05 cm diameter) and employs a high-resolution protocol. Each sample was placed in an acrylic box fitted with ridges to aid in constant positioning of the bone. Water was added to a depth of one inch to simulate an equivalent soft tissue thickness. The mid-femur region of interest was approximately 3.0 mm in length (based on magnification estimates) and 1.76 cm from the distal edge of the femur. The distal femur region of interest included the distal 7.3 mm of the bone. The co-efficient of variation for repeated measurements on the same bone for mid- and distal femur BMD was $\leq 1.5\%$.

Results are presented as means \pm SD. The statistical analyses were performed using Statview 5.0 statistical software (SAS Institute Inc., Cary, NC). Analysis of variance with Fisher's protected two-sided Least Significance Difference (LSD) test was used to perform comparisons between groups using body weights as a co-variate. $p < 0.05$ was considered significant.

Results

General observations

There were no unexpected animal deaths during this study. PGE₂ caused diarrhea and lethargy immediately after injection and these symptoms lasted for about two hours. Rats receiving Rolipram at all dose levels exhibited reduced activities for approximately 2 hours post-dosing after which they returned to normal activity levels.

Body and muscle weights (Figure 1 and Table 2)

Compared to the sham-operated rats, body and muscle weights were higher after 60 days of OVX. PGE₂ and Alendronate-treated rats had similar body and muscle weights as those of OVX animals. From 30 days to the end of the study, Rolipram 0.3-1.0 mg increased body and muscle weights by about 10% compared to OVX rats.

Histomorphometry observations

The results are summarized as follows: (1) aging effects; (2) ovariectomy effects; (3) prostaglandin E₂ effects; (4) Alendronate effects; and (5) graded doses of Rolipram effects. The latter three responses are compared to terminal 120 day-OVX, 120 day-Sham, and pre-treatment 60 day-OVX controls (Tables 3-8).

Response of the proximal tibial metaphysis (PTM)

Aging effects (Table 3). There were no significant aging changes between 6 (basal), 8 (60d-Sham) and 10 months (120d-Sham) controls.

Ovariectomy effects (Table 4). Sixty days post-OVX

resulted in cancellous bone loss, poorer architecture (decreased Tb.N and increased Tb.Sp) coupled with stimulated resorption (eroded perimeter), bone surface-based bone formation rate and remodeling (activation frequency). After 120 days OVX, there was further cancellous bone loss along with the similar select dynamic histomorphometric profiles as in 60 days post-OVX.

Prostaglandin E₂ (PGE₂) effects (Table 5). Sixty days treatment with PGE₂ resulted in increased cancellous bone mass and improved architecture (increased Tb.Wi, Tb.N, and decreased Tb.Sp) along with increased BFR/T.Ar, decreased E.Pm/B.Pm and activation frequency, compared to 120d-OVX controls. When comparing the PGE₂ group with 120d-Sham controls, the PGE₂ treated rats had a non-significant increased cancellous bone mass, but significantly increased bone formation (BFR/T.Ar and BFR/B.Pm) and activation frequency (Ac.f).

Alendronate (Ale) effects (Table 5). Sixty days of treatment with Alendronate showed increased cancellous bone and improved architecture (increased Tb.Wi and Tb.N and decreased Tb.Sp) accompanied by lower bone resorption (%E.Pm/B.Pm), bone turnover (BFR/B.Ar) and remodeling (Ac.f) compared to 120d-OVX controls.

Changes were limited to significantly decreased trabecular bone formation (BFR/B.Pm), resorption (%E.Pm/B.Pm), bone turnover (BFR/B.Ar) and remodeling (Ac.f) compared to 60d-OVX controls.

Rolipram (Rol) effects (Table 5). All doses of Rolipram exhibited more cancellous bone and better architecture (increased Tb.N and decreased Tb.Sp), a higher bone formation rate (BFR/T.Ar) along with lower %E.Pm/B.Pm and Ac.f compared to 120d-OVX controls.

When compared to 120d-Sham controls, except for the highest dose (1.0 mg/kg), cancellous bone area was lower at the other 3 lower doses (0.1, 0.3 and 0.6 mg/kg). Trabecular numbers were decreased and trabecular separations were higher at all dose levels.

The 1.0 mg/kg Rolipram dose induced a non-significantly increased cancellous bone mass and improved architecture accompanied by lower BFR/B.Ar, BFR/B.Pm, %E.Pm/B.Pm and Ac.f compared to 120d-OVX group.

Rolipram versus PGE₂ (Table 5). The 3 lower doses of Rolipram showed significantly less cancellous bone while the 1.0 mg/kg Rolipram showed a non-significant 22% reduction in bone mass compared to PGE₂ treatment.

Rolipram versus Alendronate (Table 5). The 1.0 mg/kg Rolipram treatment caused a non-significant 80% increase in cancellous bone mass existing while all other select histomorphometric parameters showed, also showed non-significant changes except for higher %E.Pm/B.Pm.

Response of the tibial shaft (TX)

Aging effects (Table 6). At 10 months of age, a total shut-down of periosteal bone formation (Ps-BFR/B.Pm) and activation of endocortical bone formation occurred compared to

Groups	Age mos.	B.Ar/T.Ar %	Tb.Wi μm	Tb.N #/mm	Tb.Sp μm	BFR/T.Ar %/y	BFR/B.Ar %/y	BFR/B.Pm $\mu\text{m}^3/\mu\text{m}^2/\text{d}\times 100$	E.Pm/B.Pm %	Ac.f cycle/y
Basal	6	11.00 \pm 1.72	39.57 \pm 0.54	2.80 \pm 0.43	323.68 \pm 52.92	36.83 \pm 2.03	335.86 \pm 31.92	21.83 \pm 2.08	4.00 \pm 0.93	0.57 \pm 0.25
60d-Sham	8	10.70 \pm 2.11	42.10 \pm 3.73	2.53 \pm 0.41	360.11 \pm 65.10	35.15 \pm 6.66	333.07 \pm 63.36	23.02 \pm 4.87	6.04 \pm 1.92	0.64 \pm 0.33
120d-Sham	10	9.29 \pm 1.76	38.59 \pm 2.40	2.39 \pm 0.32	385.57 \pm 60.43	28.74 \pm 7.37	308.52 \pm 54.31	19.54 \pm 3.45	6.10 \pm 2.13	0.40 \pm 0.15

B.Ar, bone area; T.Ar, total tissue area; Tb.Wi, trabecular width; Tb.N, trabecular number; Tb.Sp, trabecular separation; BFR, bone formation rate; B.Pm, bone perimeter; E.Pm, eroded perimeter; Ac.f, activation frequency.

Table 3. Select aging changes of the proximal tibial metaphysis (PTM).

Groups	Age mos.	B.Ar/T.Ar %	Tb.Wi μm	Tb.N #/mm	Tb.Sp μm	BFR/T.Ar %/y	BFR/B.Ar %/y	BFR/B.Pm $\mu\text{m}^3/\text{mm}^2/\text{d}\times 100$	E.Pm/B.Pm %	Ac.f cycle/y
Basal	6	11.00 \pm 1.72	39.57 \pm 0.54	2.80 \pm 0.43	323.68 \pm 52.92	36.83 \pm 2.03	335.86 \pm 31.92	21.83 \pm 2.08	4.00 \pm 0.93	0.57 \pm 0.25
60d-OVX	8	^a 5.44 \pm 1.58	46.99 \pm 12.41	^a 1.17 \pm 0.29	^a 859.97 \pm 294.39	^a 25.04 \pm 6.74	469.57 \pm 88.39	^a 34.92 \pm 3.38	^a 16.64 \pm 3.67	^a 2.26 \pm 0.95
120d-OVX	10	^{ab} 0.71 \pm 0.32	^{ab} 29.84 \pm 4.04	^{ab} 0.23 \pm 0.09	^{ab} 4858.44 \pm 2093.98	^{ab} 4.02 \pm 1.92	587.69 \pm 214.06	28.24 \pm 8.14	^a 18.33 \pm 6.07	^a 3.91 \pm 2.29

^a= p <0.05 from basal group; ^b= p <0.05 from 60 day-OVX group.

Table 4. Select ovariectomized (OVX) changes of the proximal tibial metaphysis (PTM).

Groups	B.Ar/T.Ar %	Tb.Wi μm	Tb.N #/mm	Tb.Sp μm	BFR/T.Ar %/y	BFR/B.Ar %/y	BFR/B.Pm $\mu\text{m}^3/\text{mm}^2/\text{d}\times 100$	E.Pm/B.Pm %	Ac.f cycle/y
120d-Sham	^{ab} 9.29 \pm 1.76	^b 38.59 \pm 2.40	^{ab} 2.39 \pm 0.32	^{ab} 385.57 \pm 60.43	^b 28.74 \pm 7.37	^{ab} 308.52 \pm 54.31	^a 19.54 \pm 3.45	^a 6.10 \pm 2.13	^{ab} 0.40 \pm 0.15
60d-OVX	5.44 \pm 1.58	46.99 \pm 12.41	1.17 \pm 0.29	859.97 \pm 294.39	25.04 \pm 6.74	469.57 \pm 88.39	34.92 \pm 3.38	16.64 \pm 3.67	2.26 \pm 0.95
120d-OVX	^a 0.71 \pm 0.32	^a 29.84 \pm 4.04	^a 0.23 \pm 0.09	^a 4858.44 \pm 2093.98	^a 4.02 \pm 1.92	587.69 \pm 214.06	28.24 \pm 8.14	18.33 \pm 6.07	3.91 \pm 2.29
OVX+PGE ₂	^{ab} 13.24 \pm 3.19	^{bc} 69.07 \pm 11.37	^{ab} 1.91 \pm 0.35	^b 466.12 \pm 91.59	^{abc} 45.64 \pm 8.78	^a 359.28 \pm 101.16	^c 39.54 \pm 7.83	^{ab} 6.55 \pm 1.85	^{bc} 1.03 \pm 0.34
OVX+Ale	^b 5.73 \pm 3.25	^b 42.78 \pm 3.87	^{bc} 1.29 \pm 0.62	^b 874.74 \pm 400.95	^b 12.68 \pm 13.52	^{ab} 183.19 \pm 84.77	^a 13.20 \pm 7.22	^{ab} 2.89 \pm 1.37	^{ab} 0.27 \pm 0.08
OVX+Rol-0.1	^{bcd} 4.52 \pm 2.18	^{bd} 44.16 \pm 9.63	^{bcd} 1.01 \pm 0.44	^{bcd} 1113.48 \pm 503.53	^{bd} 15.83 \pm 7.61	^c 362.85 \pm 84.73	^{ade} 25.42 \pm 3.64	^{be} 11.04 \pm 3.93	^b 1.01 \pm 0.69
OVX+Rol-0.3	^{bcd} 4.58 \pm 1.51	^{bd} 41.20 \pm 4.81	^{bcd} 1.09 \pm 0.26	^{bcd} 931.14 \pm 294.01	^{bcd} 17.38 \pm 5.11	^{be} 385.62 \pm 37.25	^{acde} 25.88 \pm 1.57	^{de} 11.93 \pm 3.06	^{abd} 0.80 \pm 0.33
OVX+Rol-0.6	^{bcd} 6.61 \pm 0.74	^{bc} 52.40 \pm 9.33	^{bcd} 1.27 \pm 0.14	^{bcd} 738.53 \pm 89.64	^{bcd} 16.94 \pm 3.92	^{ab} 254.87 \pm 42.59	^{ad} 21.78 \pm 4.25	^{abe} 9.06 \pm 1.92	^{ab} 0.87 \pm 0.53
OVX+Rol-1.0	^b 10.31 \pm 4.12	^{bc} 24.38 \pm 38.77	^{bc} 1.59 \pm 0.28	^{bcd} 576.32 \pm 90.51	^{bd} 18.79 \pm 5.70	^{ab} 208.03 \pm 86.01	^{ad} 19.46 \pm 5.27	^{abe} 7.99 \pm 3.67	^{ab} 0.69 \pm 0.41

Ale, Alendronate; Rol, Rolipram 0.1, 0.3, 0.6, 1.0 mg/kg/d, respectively; B.Ar, bone area; T.Ar, total tissue area; Tb.Wi, trabecular width; Tb.N, trabecular number; Tb.Sp, trabecular separation; BFR, bone formation rate; B.Pm, bone perimeter; E.Pm, eroded perimeter; Ac.f, activation frequency; ^a= p <0.05 from 60d-OVX; ^b= p <0.05 from 120d-OVX; ^c= p <0.05 from 120d-Sham; ^d= p <0.05 between Rolipram and PGE₂ group; ^e= p <0.05 between Rolipram and Alendronate group.

Table 5. Select histomorphometric changes of the proximal tibial metaphysis (PTM) in prostaglandin E₂ (PGE₂), Alendronate (Ale) and Rolipram (Rol)-treated ovariectomized (OVX) rats.

Groups	Age mos.	Tt.Ar mm ²	Ma.Ar mm ²	%Ct.Ar %	Ps-MAR $\mu\text{m}/\text{d}$	Ps-BFR/B.Pm $\mu\text{m}/\text{d}\times 100$	Ec-MAR $\mu\text{m}/\text{d}$	Ec-BFR/B.Pm $\mu\text{m}\times 100$	Ec-E.Pm/B.Pm %
Basal	6	4.61 \pm 0.20	0.84 \pm 0.09	81.84 \pm 2.27	0.51 \pm 0.42	12.86 \pm 10.17	0.00 \pm 0.00	0.00 \pm 0.00	4.29 \pm 0.90
60d-Sham	8	4.75 \pm 0.32	0.79 \pm 0.16	83.60 \pm 2.47	0.46 \pm 0.42	17.84 \pm 17.12	0.00 \pm 0.00	0.00 \pm 0.00	6.75 \pm 2.55
120d-Sham	10	4.86 \pm 0.22	0.93 \pm 0.17	80.86 \pm 3.00	ab0.00 \pm 0.00	ab0.00 \pm 0.00	ab0.11 \pm 0.26	ab3.05 \pm 7.48	5.75 \pm 2.42

Tt.Ar, total cross-sectional area; Ma.Ar, marrow area; Ct.Ar, cortical bone area; MAR, mineral apposition rate; BFR, bone formation rate; B.Pm, bone perimeter; E.Pm, eroded perimeter; Ps, periosteal surface; Ec, endocortical surface; ^a= p <0.05 from basal group; ^b= p <0.05 from 60 day-Sham group.

Table 6. Select aging changes of the tibial diaphysis (TX).

Groups	Age mos.	Tt.Ar mm ²	Ma.Ar mm ²	%Ct.Ar %	Ps-MAR μm/d	Ps-BFR/B.Pm μm/dx100	Ec-MAR μm/d	Ec-BFR/B.Pm μm×100	Ec-E.Pm/B.Pm %
Basal	6	4.61±0.20	0.84±0.09	81.84±2.27	0.51±0.42	12.86±10.17	0.00±0.00	0.00±0.00	4.29±0.90
60d-OVX	8	4.91±0.38	0.93±0.14	81.06±1.70	^a 1.14±0.21	^a 83.22±36.85	^a 0.62±0.50	^a 11.63±11.51	^a 15.43±5.50
120d-OVX	10	^a 5.16±0.27	^{ab} 1.19±0.12	^a 76.91±2.66	^b 0.13±0.32	^b 3.23±7.92	^a 0.72±0.24	^a 19.32±9.55	^a 13.04±5.10

^a=*p*<0.05 from basal group; ^b=*p*<0.05 from 60 day-ovx group.

Table 7. Select ovariectomy (OVX) changes of the tibial diaphysis (TX).

Groups	Tt.Ar mm ²	Ma.Ar mm ²	%Ct.Ar %	Ps-MAR μm/d	Ps-BFR/B.Pm μm/d×100	Ec-MAR μm/d	Ec-BFR/B.Pm μm×100	Ec-E.Pm/B.Pm %
120d-Sham	4.86±0.22	0.93±0.17	80.86±3.00	^{ab} 0.00±0.00	^{ab} 0.00±0.00	^b 0.11±0.26	3.05±7.48	^a 5.75±2.42
60d-OVX	4.91±0.38	0.93±0.14	81.06±1.70	1.14±0.21	83.22±36.85	0.62±0.50	11.63±11.51	15.43±5.50
120d-OVX	5.16±0.27	^a 1.19±0.12	76.91±2.66	^a 0.13±0.32	^a 3.23±7.92	0.72±0.24	19.32±9.55	13.04±5.10
OVX+PGE ₂	5.16±0.41	^b 0.70±0.28	^b 86.57±5.05	^{bc} 0.84±0.16	^{bc} 41.24±13.00	^c 0.99±0.09	^{abc} 47.62±10.99	^{abc} 1.42±1.59
OVX+Ale	4.96±0.27	^b 0.89±0.11	^b 82.07±1.47	^{bc} 0.73±0.27	^{bc} 34.83±26.37	0.45±0.37	12.58±12.12	^{ab} 3.75±2.02
OVX+Rol-0.1	^c 5.36±0.20	1.00±0.11	^b 81.41±1.66	^{abc} 0.63±0.66	^{abc} 25.10±9.62	0.63±0.36	20.49±13.99	^a 5.75±2.86
OVX+Rol-0.3	5.19±0.17	^b 0.96±0.06	^b 81.60±1.05	^{abc} 0.65±0.12	^{abc} 26.59±7.44	^{cd} 0.68±0.08	^c 22.07±8.01	^a 5.11±4.66
OVX+Rol-0.6	5.18±0.24	^b 0.98±0.09	81.10±1.71	^{abc} 0.63±0.09	^{abc} 23.21±9.33	^{cd} 0.60±0.10	^{cd} 15.93±2.72	^{ab} 4.71±2.18
OVX+Rol-1.0	5.02±0.25	0.96±1.47	^{bd} 80.82±0.08	^{abc} 0.69±0.02	^{abc} 24.16±5.08	^{cd} 0.68±0.14	^c 16.07±6.62	^{ab} 3.85±1.37

Ale, Alendronate; Rol, Rolipram 0.1, 0.3, 0.6, 1.0 mg/kg/d, respectively; Tt.Ar, total cross-sectional area; Ma.Ar, marrow area; Ct.Ar, cortical bone area; MAR, mineral apposition rate; BFR, bone formation rate; B.Pm, bone perimeter; E.Pm, eroded perimeter; Ps, periosteal surface; Ec, endocortical surface; ^a=*p*<0.05 from 60d-OVX; ^b=*p*<0.05 from 120d-OVX; ^c=*p*<0.05 from 120d-sham; ^d=*p*<0.05 between Rolipram and PGE₂ group.

Table 8. Select histomorphometric changes of the tibial diaphysis (TX) in prostaglandin E₂ (PGE₂), Alendronate (Ale) and Rolipram (Rol)-treated ovariectomized (OVX) rats.

Groups	Bone volume/tissue volume %	Trabecular thickness μm	Trabecular number 1/mm	Trabecular separation μm	Connectivity Density mm ⁻³	Cortical Thickness μm	Star Volume mm ³	Plate Derived %
Basal	^b 39.84±1.54	73.29±2.44	^b 5.44±0.21	^b 110.82±6.46	^b 95.10±10.30	^b 118.83±15.93	^b 0.13±0.04	37.38±1.82
60d-Sham	^b 39.32±1.41	^b 75.55±3.69	^b 5.21±0.18	^b 116.58±4.77	82.06±13.70	^b 187.80±11.01	^b 0.15±0.04	36.85±2.42
120d-Sham	^b 38.40±1.58	^b 74.97±4.70	^b 5.13±0.22	^b 120.23±5.50	77.79±17.1	^b 189.67±15.28	^b 0.18±0.04	36.32±1.95
60d-OVX	^b 34.46±2.23	71.41±2.67	4.83±0.32	136.41±12.99	83.44±15.50	167.83±5.04	0.30±0.09	36.58±2.41
120d-OVX	31.17±3.37	70.23±5.63	4.44±0.30	155.98±17.31	72.40±14.20	160.60±18.74	0.38±0.17	37.01±1.73
OVX+PGE ₂	^b 45.56±3.53	^{ab} 94.12±5.11	^b 4.84±0.21	^a 112.88±11.26	^a 53.00±5.70	^{ab} 200.67±11.24	^a 0.10±0.02	^a 41.71±1.40
OVX+Ale	^b 36.24±3.19	^b 75.70±2.22	^b 4.78±0.34	^b 134.24±16.29	66.40±8.34	^b 180.50±5.32	^b 0.25±0.08	38.40±1.92
OVX+Rol-0.1	^b 35.05±2.94	^{bc} 74.35±2.62	^b 4.71±0.26	^b 138.51±13.34	70.64±6.40	^{bc} 174.00±5.14	^{bc} 0.25±0.06	37.22±1.67
OVX+Rol-0.3	^b 36.00±1.50	^{bc} 75.87±2.73	^b 4.75±0.27	^b 135.17±9.90	70.08±9.71	^{bc} 178.80±8.01	^{bc} 0.21±0.07	37.87±1.35
OVX+Rol-0.6	^b 36.92±2.46	^{bc} 77.26±3.91	^b 4.78±0.17	^b 132.28±9.30	69.42±6.84	^{bc} 171.40±16.65	^{bc} 0.21±0.04	38.70±1.70
OVX+Rol-1.0	^b 38.74±2.65	^{ab} 81.05±3.07	^b 4.78±0.26	^b 128.65±12.02	67.86±10.50	^{bc} 174.60±17.77	^a 0.16±0.03	^{ab} 40.32±2.41

Ale, Alendronate; Rol, Rolipram 0.1, 0.3, 0.6, 1.0 mg/kg/d, respectively; ^a=*p*<0.05 from 60d-OVX; ^b=*p*<0.05 from 120d-OVX; and ^c=*p*<0.05 between Rolipram and PGE₂.

Table 9. Select μCT changes of the lumbar vertebrae (LV).

6 months (basal or beginning control) and 8 months (60d-Sham controls).

Ovariectomy (OVX) effects (Table 7). At 60 days post-ovariectomy (60d-OVX), the tibial shaft exhibited significantly increased periosteal and endocortical bone formation (Ps- Ec-BRF/B.Pm) and endocortical resorption (%Ec-

E.Pm/B.Pm) but no change in architectural parameters.

At 120 days post-ovariectomy (120d-OVX), there was a decrease in cortical bone (%Ct.Ar) and increases in marrow cavity (Ma.Ar) along with increases in endocortical bone resorption (Ec-E.Pm/B.Pm), reactivation of endosteal bone formation, and decreases in periosteal bone formation (Ps-

BFR/B.Pm) compared to basal or beginning controls.

Prostaglandin E₂ (PGE₂) effects (Table 8). Sixty days of PGE₂ to 60d-OVX rats induced significantly increased cortical bone (%Ct.Ar) and decreased marrow cavity (Ma.Ar) with a decrease in endocortical resorption (Ec-E.Pm/B.Pm) and increases in periosteal and endocortical bone formation compared to 120d-OVX controls.

The PGE₂-treated tibial shaft differed from the 120d-Sham controls with elevated periosteal and endocortical formation rates and decreased endocortical bone resorption.

Compared to 60d-OVX controls, the PGE₂-treated tibial shafts showed elevated endocortical bone formation and reduced bone resorption.

Alendronate (Ale) effects (Table 8). Alendronate treatment resulted in higher cortical bone area and smaller marrow cavity to exist in association with increased periosteal bone formation and reduced endocortical bone resorption compared to 120d-OVX controls.

A comparison to 120d-Sham controls found Ale differed in activating periosteal bone formation.

When compared with pre-treatment OVX'd (60d-OVX) controls, Alendronate treatment only significantly depressed endocortical bone resorption.

Rolipram (Rol) effects (Table 8). Sixty days' treatment with all doses of Rolipram found more cortical bone and less marrow area together with increased periosteal bone formation and decreased endocortical bone resorption compared to 120d-OVX controls.

Compared to 120d-Sham controls, Rolipram treatment differed by increasing periosteal and endocortical bone formation. Rolipram significantly decreased periosteal bone formation compared to 60d-OVX controls.

Rolipram versus PGE₂ (Table 8). Rolipram differed only in significantly reduced endocortical bone formation. There was a significant 7% reduction in cortical bone mass with Rolipram.

Rolipram versus Alendronate (Table 8). No differences were found between the two treatments.

Lumbar vertebral μ CT (Table 9)

One hundred and twenty days of ovariectomy significantly decreased trabecular bone volume, trabecular number, and cortical thickness compared to all sham control groups. PGE₂ treatment significantly increased trabecular and cortical thickness compared to the 60d and 120d-OVX groups. Alendronate treatment had similar bone volume compared to the 60d-OVX group. Rolipram treatment at 0.1-0.6 mg dose levels had similar trabecular bone volume and trabecular thickness compared to the 60d-OVX group. Trabecular thickness and plate-like trabeculae were increased in the 1.0 mg Rolipram dose group compared to the 60d-OVX group.

Femur DEXA (Figures 2 and 3)

Ovariectomy significantly decreased distal femur areal BMD and BMC compared to the sham control groups. PGE₂

significantly increased mid- and distal femur areal BMD and BMC compared to OVX groups. Alendronate had similar areal BMD and BMC in the mid- and distal femur as the 60d-OVX group. Rolipram had similar areal BMD and BMC at the distal femur as the 60d-OVX group. At the 1 mg dose level, Rolipram significantly increased mid-femur BMD compared to the 120d-OVX group. At all doses, Rolipram had lower areal BMD level than PGE₂ at both the mid- and distal femur.

Discussion

The results of this study indicated that daily administration of Rolipram, a PDE4-specific inhibitor, prevented further bone loss in an adult established osteopenia model. These findings were consistent in five skeletal sites that were measured: tibial metaphysis and diaphysis, lumbar vertebra body, distal femur metaphysis and femoral diaphysis. A dose-response effect was seen in the trabecular bone compartments in the proximal tibial metaphysis and the lumbar vertebral body. Dynamic bone histomorphometry suggested that these beneficial effects were achieved by partially maintaining the elevated bone formation at the trabecular bone surface and at the periosteal bone surface. Furthermore, it decreased bone turnover and at the 0.6 and 1.0 mg/kg Rolipram dose levels on the trabecular surfaces and at all dose levels on the endocortical bone surfaces. The prevention of further effects of bone loss were comparable to those of an antiresorption agent (Alendronate) but were not as great as those of an anabolic agent (PGE₂).

In contrast to the relative high doses (1-30 mg/kg) used in other studies^{19,21}, we chose to lower Rolipram doses to evaluate if we could prevent further bone loss or restore cancellous bone in rats with established osteopenia. Bone histomorphometry performed at the tibial metaphysis and diaphysis clearly showed that Rolipram affected both the periosteal and endosteal envelopes. Rolipram was effective in preventing further cancellous bone loss associated with estrogen-depletion started from the lowest dose level. It maintained all the static parameters (bone mass and architecture) at the pre-treatment level accompanied by slightly decreasing bone formation and decreasing the elevated bone resorption, bone turnover and remodeling induced by ovariectomy. Both animal studies and human data tend to support that there is an inverse relationship between bone mass and bone turnover, and decreased bone strength and/or fractures are likely linked to increased bone turnover²⁶⁻²⁹. We suspect that decreased bone turnover and remodeling could contribute to increased bone strength and decreased fracture risk. Although Rolipram treatment was not as potent as those of PGE₂ in restoring bone mass, it was comparable to those of Alendronate with regard to the prevention of further OVX-induced bone loss when the dose was used at a level greater than 0.6 mg/kg.

When rats are ovariectomized at the age of 3 to 10 months, periosteal bone modeling drifts are usually

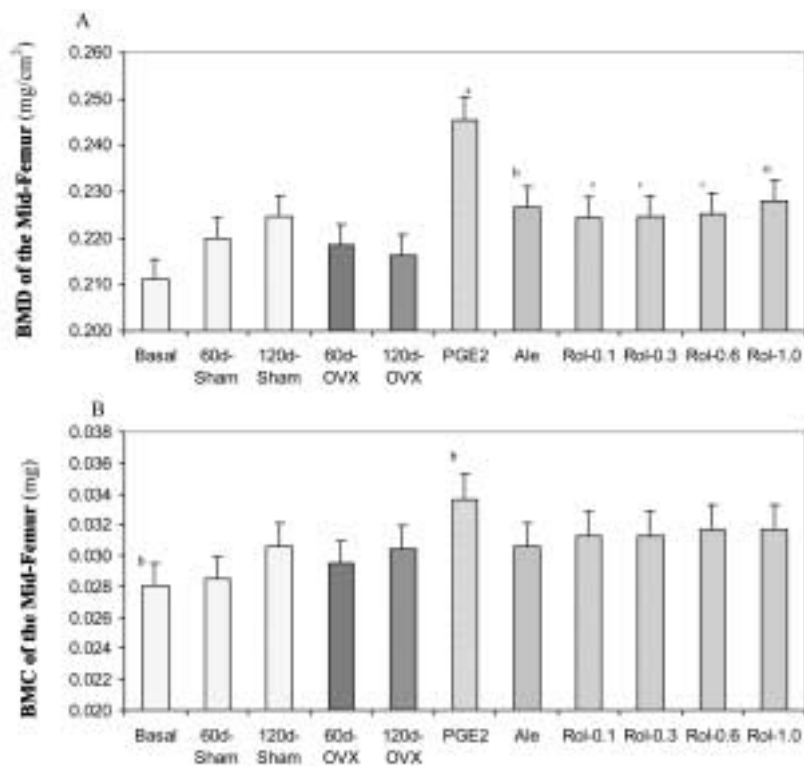


Figure 2. Bone mineral density (BMD, A) and bone mineral content (BMC, B) of the mid-femur. PGE₂, Alendronate and Rolipram at 1.0 mg/kg increased BMD compared to final OVX group. Only PGE₂ increased BMC. ^a=*p*<0.05 from 60d-OVX; ^b=*p*<0.05 from 120d-OVX; and ^c=*p*<0.05 between Rolipram and PGE₂ group.

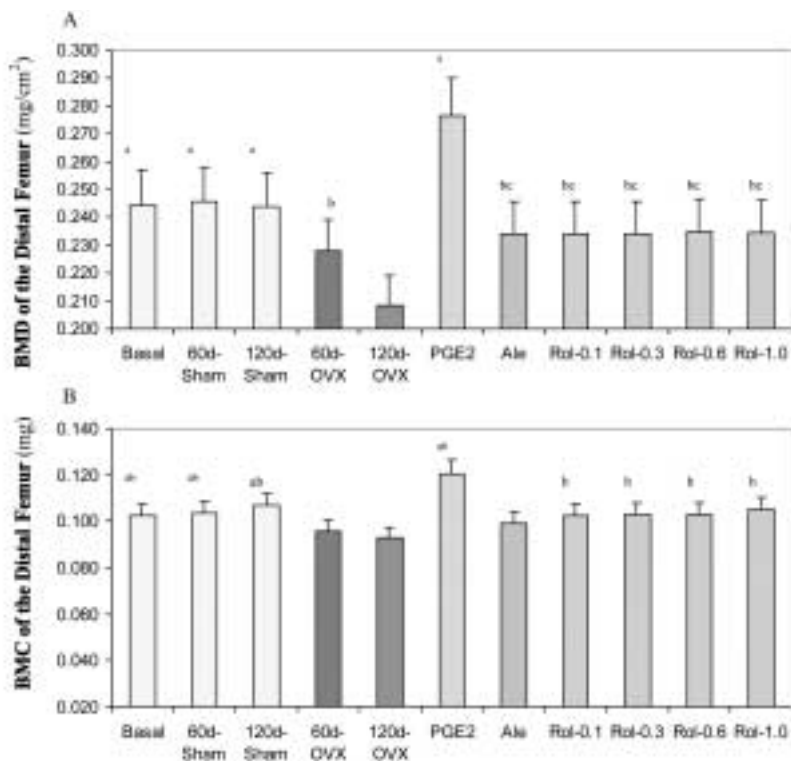


Figure 3. Bone mineral density (BMD, A) and bone mineral content (BMC, B) of the distal femur. Ovariectomy decreased distal femur BMD and BMC. PGE₂ increased both BMD and BMC. Alendronate prevented the decrease of BMD. Rolipram at all doses prevented further decreases of BMD and BMC. ^a=*p*<0.05 from 60d-OVX; ^b=*p*<0.05 from 120d-OVX; and ^c=*p*<0.05 between Rolipram and PGE₂ group.

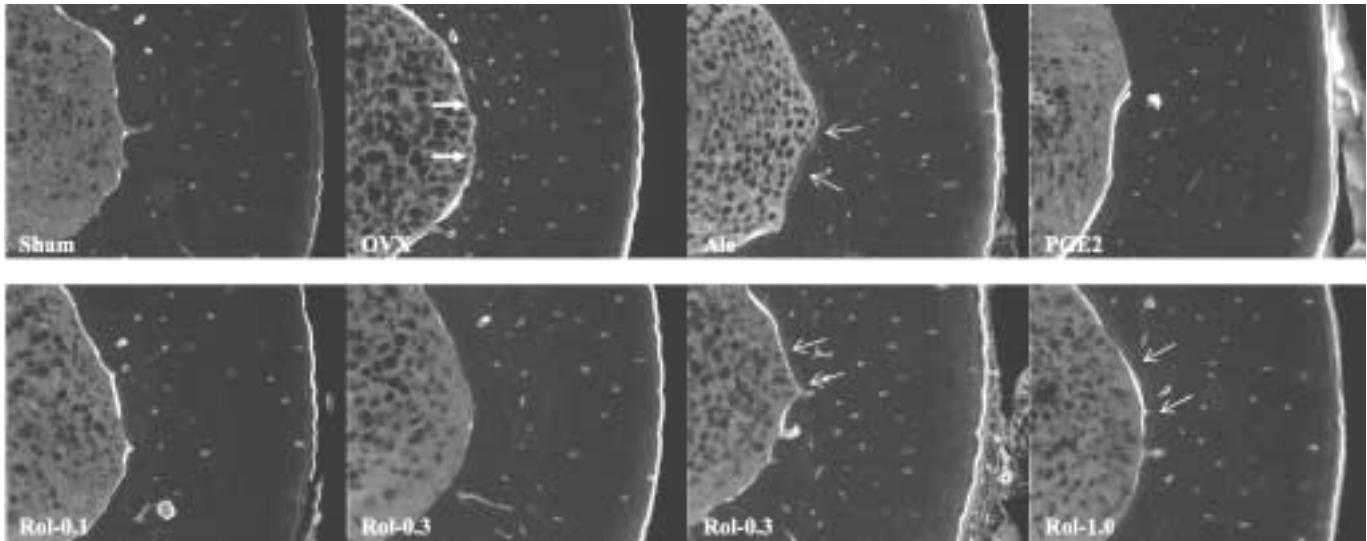


Figure 4. Cortical bone of the tibial diaphysis at 120 days. Ovariectomy increased endocortical bone eroded (white arrows) and periosteal bone formation. Alendronate inhibited endocortical bone resorption as is evident by the decrease of eroded surface and preservation of the pre-treatment Xylenol Orange label (orange label, white arrows). PGE₂ increased double labels at both the periosteal and endocortical surfaces; cortical width was increased. Rolipram at all four doses had similar periosteal labeling as the OVX group but had less endocortical bone eroded surface. Pre-treatment Xylenol Orange label (arrows) could be seen in the two highest dose groups. Original magnification: 60 \times .

enhanced or reactivated. This increased periosteal expansion will compensate for the endocortical bone loss and results in no decrease in cortical thickness at least for 6 months post-OVX. As expected, we found that OVX induced a transient increase in periosteal apposition but returned to near aging control level in 4 months. Cortical bone area began to decrease by the end of the study (Table 7). However, in the Rolipram-treated ovariectomized animals, periosteal bone formation was enhanced at a level that was above aging control level. As a result, cortical bone area and cortical thickness did not decrease (Figure 4). The periosteal mineral apposition rates were partially sustained while the endocortical apposition rates were maintained by Rolipram treatment. This may result in an increase in bone strength as the new bone is added to the periosteal surface where it has the greater biomechanical impact.

Micro-CT measurement not only allowed us to observe bone volume, but also allowed us to follow the changes of bone architecture. Trabecular architecture deteriorations were found after 4 months of estrogen depletion in the lumbar vertebral bodies of the rats as shown by the decreases of bone volume, trabecular number, thickness and increases of trabecular separation and star volume. Cortical bone thickness was also found to be decreased after OVX. Rolipram prevented OVX-induced decrease of the trabecular number, and the lower trabecular separation and star volume pointed to its ability to preserve bone connectivity. It also increased trabecular thickness, inducing more plate-like trabeculae, which may increase the lumbar load-bearing strength as trabecular thickness correlated well with ultimate compressive

strength in the lumbar vertebrae³⁰⁻³². Furthermore, because cortical bone may play a larger role in determining the strength of the lumbar vertebra than the trabecular bone^{32,33}, Rolipram treatment may presumably prevent the decrease in bone biomechanical properties following OVX by preventing cortical bone loss in the lumbar vertebrae. However, we will need to perform additional whole bone biomechanical testing to verify our speculations.

DEXA measurements on the femur demonstrated, that like Alendronate, Rolipram increased bone density without affecting bone mineral content of the mid-shaft when employed at the highest dose level (1.0 mg/kg). This suggests that the effects of Rolipram on this bone site were anti-resorptive. In the distal femur, a site dominated by cancellous bone, Rolipram maintained both bone mineral density and content at pre-treatment levels. Although bone mineral density of the Rolipram-treated groups was similar to that of Alendronate-treated group, they had higher bone mineral content than that of Alendronate, suggesting Rolipram employed at the level of 1.0 mg/kg might have better anti-resorptive effects compared to that of Alendronate.

It was reported that the deterioration of trabecular bone structure in long bone (proximal tibia) following estrogen depletion results from the conversion of plate to rod elements due to the perforation of the trabecular plates and the loss of bone connectivity³⁴. This loss of connectivity was irreversible even if bone volume was restored to the baseline level with estrogen replacement or with anabolic treatment. However, the vertebral μ CT data indicated that OVX did not induce the loss of connectivity density despite the losses of trabecular bone vol-

ume and number; PGE₂, Alendronate and Rolipram treatments tended to have lower connectivity density than ovariectomized animals, even though these treatments restored the trabecular bone volume. The discrepancy of initial change of bone connectivity between the proximal tibial and the vertebra may be due to the presence of more plate-like trabecular structure in the vertebra than in the proximal tibia. The initial response to estrogen depletion in the vertebra is fenestration of plates followed by their progressive enlargement that converted plates to rods, resulting in an increase in connectivity density. As three-dimensional measurements of connectivity quantify the holes in the trabecular lattice, fenestration of a plate increases the number of holes, while anabolic treatments could fill in small plate fenestrations. As a result, OVX may seem to initially increase the connectivity density while the anti-resorptive and anabolic agents may do the opposite in this particular bone site³⁵⁻³⁹. But we have to keep in mind that bone loss occurs at a slower rate in the vertebra than in the tibia: four months of ovariectomy only induced 20% loss of cancellous bone in the vertebra versus over 80% in the proximal tibia⁴⁰⁻⁴¹. If the experimental period were prolonged so that the vertebra developed severe osteopenia, it would be possible that we could see the loss of trabecular connectivity density in this bone site.

One unexpected but interesting finding in this study is that higher doses of Rolipram rapidly increased body weights when it was initiated and increased muscle weights (Figure 1 and Table 2) without significantly affecting other organ weights (data not shown). The mechanisms underlining these changes were unknown. It has been proposed and seems to be true that muscle force is the main determinant of the post-natal and whole-bone strength and bone "mass"⁴²⁻⁴⁴. In our previous studies, we found that the loss of muscle weight preceded the bone loss and the recovery of muscle preceded the recovery of bone mass⁴⁵. Similar results also occur in humans⁴⁶⁻⁴⁸. The increases in muscle and body weight by Rolipram may contribute to maintaining the elevated periosteal bone formation and inhibit endosteal bone resorption. Further evaluations on the function of the muscles are necessary before we could substantiate this conclusion.

Inhibitors of PDE4 act by increasing intracellular concentrations of cyclic AMP, which have a broad range of anti-inflammatory effects on various key effector cells involved in asthma and chronic obstructive pulmonary disease (COPD). The therapeutic ratio for PDE4 inhibitors is thought to be determined by selectivity on receptor subtypes for the relative effects on PDE4B (anti-inflammatory) and PDE4D (emesis). The main side effects of PDE4 inhibitors include central nervous and gastrointestinal side effects, which have limited their clinical application⁴⁹. Since rats in general do not vomit, we are not surprised to see the lack of emesis following Rolipram administration. Further toxicology study in larger animals will be necessary for this purpose.

In summary, the present study has shown that Rolipram, a PDE4 inhibitor, prevented OVX-induced bone loss at all five skeletal sites tested. A dose-response effect was seen in the trabecular bone compartments in the proximal tibial metaphysis

and the lumbar vertebral body. Maintaining the ovariectomy-elevated bone formation at both the periosteal and endosteal surfaces but inhibiting endosteal bone resorption and lowering bone turnover may account for the static changes. The prevention of further bone loss effects of Rolipram were comparable to those of Alendronate with regards to bone mass and bone resorption. Developing a PDE4 analog that could eliminate their unpleasant side effects but would sustain its beneficial effects on the skeleton is an attractive idea of drug development for the treatment of osteoporosis.

References

1. World Health Organization Assessment of fracture risk and its application to screening for postmenopausal osteoporosis. Report of a WHO study group. World Health Organ Tech Rep Ser 1994; 843:1-129.
2. Delmas PD. Hormone replacement therapy in the prevention and treatment of osteoporosis. *Osteoporos Int* 1997; 7:S3-S7.
3. Fleisch HA. Bisphosphonates: pre-clinical aspects and use in osteoporosis. *Ann Med* 1997; 29:55-62.
4. Lindsay R, Cosman F. Skeletal effects of estrogen analogs. *Osteoporos Int* 1997; 7:S40-S42.
5. Sogaard CH, Mosekilde L, Thomsen JS, Richards A, McOsker JE. A comparison of the effects of two anabolic agents (fluoride and PTH) on ash density and bone strength assessed in an osteopenic rat model. *Bone* 1997; 20:439-449.
6. Ke HZ, Jee WSS, Mori S, Li XJ, Kimmel DB. Effects of long-term daily administration of prostaglandin E₂ on maintaining elevated proximal tibial metaphyseal cancellous bone mass in male rats. *Calcif Tissue Int* 1992; 50:245-252.
7. Lane NE, Yao W, Kinney JH, Modin G, Balooch M, Wronski TJ. Both hPTH(1-34) and bFGF increase trabecular bone mass in osteopenic rats but they have different effects on trabecular bone architecture. *J Bone Miner Res* 2003; 18:2105-2115.
8. Beavo JA. Cyclic nucleotide phosphodiesterases: functional implications for multiple isoforms. *Physiol Rev* 1995; 75:725-748.
9. Conti M, Nemoz G, Sette C, Vicini E. Recent progress in understanding the hormonal regulation of phosphodiesterases. *Endocr Rev* 1995; 16:370-389.
10. Besse A, Trimoreau F, Faucher JL, Praloran V, Denizot Y. Prostaglandin E₂ regulates macrophage colony stimulating factor secretion by human bone marrow stromal cells. *Biochim Biophys Acta* 1999; 13:444-451.
11. Kaneki H, Takasugi I, Fujieda M, Kiri M, Mizuochi S, Ide H. Prostaglandin E₂ stimulates the formation of mineralized bone nodules by a cAMP-independent mechanism in the culture of adult rat calvarial osteoblasts. *J Cell Biochem* 1999; 73:36-48.
12. Yu XP, Chandrasekhar S. Parathyroid hormone (PTH

- 1-34) regulation of rat osteocalcin gene transcription. *Endocrinology* 1997; 138:3085-3092.
13. Yu XP, Chandrasekhar S. Rapid protein kinase A-mediated activation of cyclic AMP-phosphodiesterase by parathyroid hormone in UMR-106 osteoblast-like cells. *J Bone Miner Res* 1997; 138:172-178.
 14. Koh AJ, Beecher CA, Rosol TJ, McCauley LK. 3',5'-Cyclic adenosine monophosphate activation in osteoblastic cells: effects on parathyroid hormone-1 receptor and osteoblastic differentiation *in vitro*. *Endocrinology* 1999; 140:3154-3162.
 15. Soderling SH, Beavo JA. Regulation of cAMP and cGMP signaling: new phosphodiesterases and new functions. *Curr Opin Cell Biol* 2000; 12:174-179.
 16. Reneland RH, Mah S, Kammerer S, Hoyal CR, Marnellos G, Wilson SG, Sambrook PN, Spector TD, Nelson MR, Braun A. Association between a variation in the phosphodiesterase 4D gene and bone mineral density. *BMC Med Genet* 2005; 7:6-9.
 17. Miyamoto K, Waki Y, Horita T, Kasugai S. Reduction of bone loss by denbufylline, an inhibitor of phosphodiesterase. *Biochem Pharmacol* 1997; 54:613-617.
 18. Kasugai S, Miyamoto K, Waki Y, Mukohyama H, Kondo H, Ohya A. A phosphodiesterase IV inhibitor, Rolipram, increases osteoprogenitors in rat bone marrow. *J Bone Miner Res* 1997; 12(Suppl.1):S476.
 19. Kinoshita T, Kobayashi S, Ebara S, Yoshimura Y, Horiuchi H, Tsutsumimoto T, Wakabayashi S, Takaoka K. Phosphodiesterase inhibitors, Pentoxifylline and Rolipram, increase bone mass mainly by promoting bone formation in normal mice. *Bone* 2000; 27:811-817.
 20. Cho ES, Yu JH, Kim MS, Yim M. Rolipram, a phosphodiesterase 4 inhibitor, stimulates inducible cAMP early repressor expression in osteoblasts. *Yonsei Med J* 2005; 46:149-154.
 21. Waki Y, Horita T, Miyamoto K, Ohya K, Kasugai S. Effects of XT-44, a phosphodiesterase 4 inhibitor, in osteoblastogenesis and osteoclastogenesis in culture and its therapeutic effects in rat osteopenia models. *Jpn J Pharmacol* 1999; 79:477-483.
 22. Parfitt AM, Drezner MK, Glorieux FH, Janis JA, Malluche H, Meunier PJ, Ott SM, Recker RR. Bone histomorphometry: standardization of nomenclature, symbols and units. Report of the ASBMR Histomorphometry Committee. *J Bone Miner Res* 1987; 2:595-610.
 23. Parfitt AM, Matthews CHE, Villanueva AR, Kleerekoper M, Frame B, Rao DS. Relationships between surface, area, and thickness of iliac trabecular bone in aging and in osteoporosis. *J Clin Invest* 1983; 72:1396-1409.
 24. Jee WSS, Inoue J, Jee KW, Haba T. Histomorphometric assay of the growing long bone. In: Takahashi H (ed) *Handbook of Bone Morphology*. Niigata City, Nishimura, Japan 1983; 101-103.
 25. Laib A, Kumer JL, Majumdar S, Lane NE. The temporal changes of trabecular architecture in ovariectomized rats assessed by microCT. *Osteoporos Int* 2001; 12:936-941.
 26. Garnero P, Hausherr E, Chapuy MC, Marcelli C, Grandjean H, Muller C, Cormier C, Breart G, Meunier PJ, Delmas PD. Markers of bone resorption predict hip fracture in elderly women: the EPIDOS prospective study. *J Bone Miner Res* 1996; 11:1531-1538.
 27. Garnero P, Sornay-Rendu E, Chapuy M-C, Delmas PD. Increased bone turnover in late postmenopausal women is a major determinant of osteoporosis. *J Bone Miner Res* 1996; 10:337-349.
 28. Marshall D, Johnell O, Wedel H. Meta-analysis of how well measures of bone mineral density predict occurrence of osteoporotic fracture. *BMJ* 1996; 312:1254-1259.
 29. Minisola S, Pacitti MT, Ombriccolo E, Costa G, Scarda A, Palombo E, Rosso R. Bone turnover and its relationship with BMD in pre- and postmenopausal women with or without fractures. *Maturitas* 1998; 29:265-270.
 30. Dempster DW, Ferguson-Pell MW, Mellish RWE, Cochran GVB, Xie F, Fey C, Horbert W, Parisien M, Lindsay R. Relationship between bone structure in the iliac crest and bone structure and strength in the lumbar spine. *Osteoporos Int* 1993; 3:90-96.
 31. Mosekilde L, Danielsen CC, Sogaard CH and Thorling E. The effect of long-term exercise on vertebral and femoral bone mass, dimensions, and strength-assessed in a rat model. *Bone* 1994; 15:292-301.
 32. Rockoff SD, Sweet E, Bluestein J. The relative contribution of trabecular and cortical bone to the strength of human lumbar vertebrae. *Calcif Tissue Res* 1969; 3:163-175.
 33. Vesterby A, Mosekilde Li, Gundersen HJG, Melsen F, Mosekilde Le, Holme K, Sorensen L. Biological meaningful determinations of the *in vitro* strength of lumbar vertebra. *Calcif Tissue Int* 1991; 48(Suppl):A71.
 34. Lane NE, Thompson JM, Haupt D, Kimmel DB, Modin G, Kinney JH. Acute changes in trabecular bone connectivity and osteoclast activity in the ovariectomized rat *in vivo*. *J Bone Miner Res* 1998; 13:229-236.
 35. Mosekilde L, Danielsen CC, Gasser JA. The effects on vertebral bone mass and strength of long-term treatment with anti-resorptive agents (Estrogen and Calcitonin), human parathyroid hormone (1-38), and combination therapy, assessed in aged ovariectomized rats. *Endocrinology* 1994; 134:2126-2134.
 36. Lane NE, Thompson JM, Stewler GJ, Kinney JH. Intermittent treatment with human parathyroid hormone (hPTH[1-34]) increased trabecular bone volume but not connectivity in osteopenic rats. *J Bone Miner Res* 1995; 10:1470-1477.
 37. Lane NE, Haupt D, Kimmel DB, Modin G, Kinney JH. Early estrogen replacement therapy reverses the rapid loss of trabecular bone volume and prevents further deterioration of connectivity in the rat. *J Bone Miner Res* 1999; 14:206-214.
 38. Boyce RW, Wronski TJ, Ebert DC, Stevens ML, Paddock CL, Youngs TA, Gundersen HJ. Direct stere-

- ological estimation of three-dimensional connectivity in rat vertebrae: effect of estrogen, etidronate, and risedronate following ovariectomy. *Bone* 1995; 16:209-213.
39. Kinney JH, Haupt DL, Balooch M, Ladd AJC, Ryaby JT, Lane NE. Three-dimensional morphometry of the L6 vertebra in the ovariectomized rat model of osteoporosis: biomechanical implications. *J Bone Miner Res* 2000; 15:1981-1991.
 40. Wronski TJ, Dann LM, Horner SL. Time course of vertebral osteopenia in ovariectomized rats. *Bone* 1989; 10:295-301.
 41. Wronski TJ, Dann LM, Scott KS, Cintrón M. Long-term effects of ovariectomy and aging on the rat skeleton. *Calcif Tissue Int* 1989; 45:360-366.
 42. Doyle F, Brown J, Lachance C. Relation between bone mass and muscle weight. *Lancet* 1970; 295:391-393.
 43. Burr DB. Muscle strength, bone mass and age-related bone loss. *J Bone Miner Res* 1997; 12:1547-1551.
 44. Frost HM, Ferretti JL, Jee WSS. Perspective: Some roles of mechanical usage, muscle strength, and the mechanical in skeleton physiology, disease, and research. *Calcif Tissue Int* 1998; 62:1-7.
 45. Yao W, Jee WSS, Chen JL, Liu HY, Tam CS, Cui L, Zhou H, Setterberg RB, and Frost HM. Making rats rise to erect bipedal stance for feeding partially prevented orchidectomy-induced bone loss and added bone to intact rats. *J Bone Miner Res* 2000; 15:1158-1168.
 46. Ferretti JL, Capozza RF, Cointy GR, Garcia SL, Plotkin H, Alvarez-Fihueira ML, Zanchetta JR. Gender-related differences in the relationship between densitometric values of whole-body bone mineral content and lean body mass in humans between 2 and 87 years of age. *Bone* 1998; 22:683-690.
 47. Schiessl H, Willnecker J, Niemeyer GT. Muscle cross-sectional area and bone cross-sectional area in the human lower leg measured with peripheral computed tomography. In: *Third International Congress on Osteoporosis*. Xian, China 1999:79-83.
 48. Schönau E. The development of the skeletal system in children and the influence of muscular strength. *Hormone Res* 1998; 12:27-31.
 49. Dyke HJ, Montana JG. Update on the therapeutic potential of PDE4 inhibitors. *Expert Opin Investig Drugs* 2002; 11:1-13.